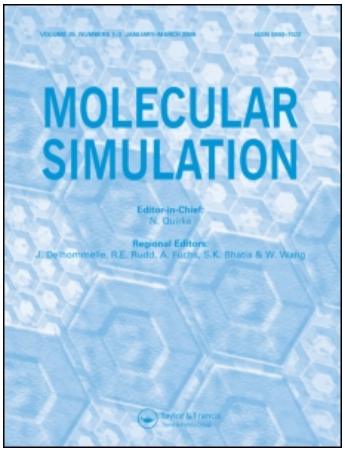

Molecular Simulation
Publication details, including instructions for authors and subscription information:
http://www.informaworld.com/smpp/title~content=t713644482

Brownian Dynamics Simulations of Domain Growth in Lennard-Jones Fluids

J. F. M. Lodge[a]; D. M. Heyes[a]
[a] Department of Chemistry, University of Surrey, Guildford

To cite this Article Lodge, J. F. M. and Heyes, D. M.(1996) 'Brownian Dynamics Simulations of Domain Growth in Lennard-Jones Fluids', Molecular Simulation, 18: 3, 155 — 177
To link to this Article: DOI: 10.1080/08927029608024121
URL: http://dx.doi.org/10.1080/08927029608024121

Molecular Simulation, 1996, Vol. 18, pp. 155–177
Reprints available directly from the publisher
Photocopying permitted by license only

BROWNIAN DYNAMICS SIMULATIONS OF DOMAIN GROWTH IN LENNARD-JONES FLUIDS

J. F. M. LODGE and D. M. HEYES

Department of Chemistry, University of Surrey, Guildford, GU2 5XH

(Received April 1996; accepted May 1996)

The evolution of the structural, thermodynamic and rheological properties of a three dimensional Lennard-Jones fluid is followed as it is quenched from a supercritical state into the two phase gas-liquid coexistence region of the phase diagram. Domain growth is revealed in the appearance of a peak in the structure factor at $k_{max} \sim \sigma_{LJ}^{-1}$ which moves to lower k with time, and whose peak height $S(k_{max})$ increases with time. k_{max}^{-1} and $S(k_{max})$ show a power law dependence with time with exponents in the range 0.2–0.3 and 0.7–1.0, respectively, depending somewhat on the destination state point and broadly consistent with previous theory and simulation. The kinetics of domain growth depends on the value of temperature and density quenched to in the two-phase region. For quenches close to the liquid-vapour coexistence line, an initial period marked by a lack of growth in the low k peak ('latency') is followed by power law behaviour, which is indicative of growth by nucleation. Quenches to well inside the unstable region are marked by classical spinodal decomposition power law growth. The influence of the box size on the phase separation has been investigated by carrying out simulations with $N = 256$ and $N = 864$. We have shown that system size can have a pronounced effect on growth kinetics, and that at least $N \geqslant 864$ are advisable for studies of this kind. Small system sizes tend to promote latency at short times and rapid phase separation at later times.

Network formation found at intermediate times is manifest in a slowing down in relaxation processes which is reflected in a decrease in the self-diffusion coefficient and increase in shear viscosity with time from the start of the quench.

Keywords: 3D Lennard-Jones; nucleation; spinodal decomposition; viscoelasticity; Brownian dynamics computer simulation

1. INTRODUCTION

When a system is quenched into the two phase region of the phase diagram, the system is initially in a non-equilibrium uniform density structurally homogeneous state. The particles eventually phase separate into two

coexisting phases with concentrations of the two phases given by the lever rule. Separation proceeds in time via spatial density fluctuations until a two phase state in thermodynamic equilibrium is formed. The mechanism of domain growth, and its dependence on the destination state point in the non-equilibrium region of the phase diagram is still poorly understood, as is the relationship between these structural changes and associated physical properties, such as rheology.

Current theories are concentrated in two areas–the mean field, MF, theoretical approach and cluster dynamical, CD, models. In the MF approach two types of instability are distinguished which characterise the early stages of phase separation, ocurring in separate regions of the phase diagram. In the metastable region, which occurs just inside the two-phase boundary, there is an instability to short wavelength finite amplitude density fluctuations. This produces decomposition via a nucleation and growth mechanism. A critical droplet size exists in this region such that transiently formed small droplets via local density fluctuations eventually disintegrate and only droplets which reach the critical size can grow. The free energy barrier to nucleation means that the nucleation rate is often very slow, so the system can exist in the one phase state for quite a long time. This can be seen in the structure factor as a small angle scattering peak which does not appear immediately, but only after a period of time ('latency'). The rate of creation of droplets is described by homogeneous nucleation theory [1].

If the system is quenched further into the centre of the two phase region, the system separates by a process termed spinodal decomposition. This is driven by an instability to long wavelength density fluctuations of infinitesimal amplitude. Phase separation is instantaneous following the quench since there is no critical droplet size and no energy barrier. The basis of mean field theories of nucleation and spinodal decomposition is a coarse grained Helmholz free energy functional, usually taken to be given by the Ginzburg-Landau form. The models use a time-dependent probability distribution functional, often a Fokker-Planck equation, or alternatively given in terms of non-linear Langevin equations for the macroscopic variables of interest. Mean field theories work best when large correlation lengths and long time scales are involved, which is typically in the immediate vicinity of the critical point. Mean-field theories, such as the Cahn-Hilliard theory, predict an activation energy which decreases monotonically to zero at the mean field spinodal. The critical droplet radius diverges at the coexistence curve and at the spinodal, and the characteristic length of the system also diverges as the spinodal is approached from the unstable region. Thus a sharp transition exists between the two regions.

For spinodal decomposition, Cahn assumed that for very short times after a quench, concentration fluctuations would be small enough to allow linearisation of a generalised non-linear diffusion equation. Using this model, Cahn predicted that long-wavelength fluctuations should grow exponentially with time, the so-called long-wavelength instability [1]. If this result is transferred to the time evolution of the structure factor, it predicts an exponential increase in the scattering intensity for $k < k_c$ with a peak at a *time-independent* wavenumber, k_m, until non-linear effects limit the growth. The exponential increase in the scattering intensity has been found in some simulations [1,2,3,5]; however, other simulations have found that coarsening behaviour starts at the shortest of measurable times, and there is no linear regime [4]. It is possible that the region where the system can be approximated linearly is too small to be seen on experimental timescales.

Whichever mechanism occurs in the early stages of phase separation, once the equilibrium fractions of phases in their final volume fraction are formed, a more widely accepted coarsening process is thought to take place, in which the finely dispersed phases coalesce into large, more sharply defined separate phases. The Lifshitz-Slyozov mechanism is developed from a mean-field approach and has been found to describe later stages of the coarsening during phase separation rather well in both experimental studies and in computer simulations [1,2,4,5,6]. The theory describes an evaporation/condensation growth mechanism for systems with low volume fractions and low supersaturation. Coarsening is assumed to occur only after nearly equilibrium volume fractions of phases have formed via single particle diffusion from smaller droplets which are dissolving to the larger growing droplets. The theory results in an average cluster size which grows with a time dependence of $R(t) \sim t^{1/3}$, where R is the average cluster radius. This result is independent of dimension and volume fraction (for small volume fractions). The Lifshitz-Slyozov $t^{1/3}$ behaviour can also be found from a cluster dynamics treatment [7].

Cluster dynamical, CD, theories describe cluster growth in terms of diffusion and reaction of clusters. As they rely on a detailed specification of clusters (which is not necessary in meanfield theories) these methods are best used at low temperatures and volume fractions where well-defined clusters exist. To date the cluster dynamical approach has been rather qualtitative owing to the problems of cluster definition, especially at later times when the clusters are large [1]. In CD theory there is no sharp distinction between metastable and unstable states. Instead, there is a gradual and smooth transition between the two types of decomposition. The activation energy decreases through the metastable region, but instead of

reaching zero, as in MF theories, it becomes of the order $k_B T$ at the MF spinodal and throughout the unstable region. The critical droplet radius and the characteristic length, k_c^{-1}, also decrease smoothly as the spinodal is approached and remain finite throughout the spinodal region [7]. This diffuse transition between phase separation mechanisms is often what is found experimentally [8].

A problem with associating power law growth behaviour with a particular mechanism is that several competing mechanisms may be taking place simultaneously. The growth exponent would therefore be expected to change with time, as different mechanisms dominate during the course of the phase separation. This has been seen in experiments as exponents cross-over from one value to another [1, 2, 6, 9]. If the volume fraction is greater than the percolation limit, a connected morphology allows growth driven by surface tension which drives fluid from the necks of the interconnected structure to bulges, leading to a $k_{max} \sim t^{-1}$ growth law, thus predicting a cross-over from diffusive growth giving a $t^{1/3}$ rate to surface tension driven growth at later time with a t^{-1} rate [10]. The addition of surfactants to two phase systems can effectively freeze the phase separation in the later stages by reducing the surface tension so there is no driving force for separation [11]. This results in a slow logarithmic growth law of $k_{max}^{-1} \sim (\ln(t))^{\theta}$. This 'freezing' of the separation process has also been seen in systems with quenched disorder [9] and with quenched impurities [12]. A similar effect is sometimes seen in the phase separation of colloid liquids. If the system reaches a point when a cluster spans the whole of the system, a metastable gel-like phase is formed in which diffusion of the particles, and thus phase separation, although not completely arrested is significantly reduced. These gel phases can exist for very long periods of time before restructuring processes finally lead to their collapse [5, 13].

Lattice-based Monte Carlo simulation has proved to be a useful method for exploring domain growth in the two-phase region [9]. However, as with all Monte Carlo methods, there is no rigorous concept of time in the technique, and therefore its application to a time dependent phenomenon, such as spinodal decomposition, should perhaps be treated with some caution. Molecular dynamics, which does rigorously follow a time-ordered series of states, has been applied in two dimensions and three dimensions to phase separation of Lennard-Jones type molecular systems [3, 4].

Colloidal liquids in which the colloidal particles interact with significant attractive interactions manifest spinodal decomposition. In these systems, the relaxation times scale as the cube of the particle diameter, so that this process can be rather long-lived on a human time scale. To date, Brownian

Dynamics, BD, has not been used to investigate spinodal decomposition in model colloidal liquids, although the analogy between the spinodal effect and gel formation in such systems has recently been explored [2] using a DLCA model. The advantage of the BD method for studying colloidal phase separation is that the dynamics are more appropriate to this class of chemical system. BD is an 'off-lattice' technique and therefore has the resolution to explore the effect of interaction potential strength and range on associated physical properties of the dynamically evolving system. The disadvantage of the technique is that it is confined to relatively small systems and short times when compared with lattice simulation techniques. Nevertheless, these limitations are not too serious as we will demonstrate below.

In order to explore the usefulness of BD in investigating phase separation with model colloidal liquids, we have carried out simulations of 3D Lennard-Jones, LJ, model colloidal liquids quenched into the two-phase part of the phase diagram. The LJ has been used because its phase diagram is now known very well ([14, 15]); also the analytic form is not unrealistic for some colloidal systems. Recent critical point values for the $r = 2.5\sigma$ truncated LJ molecule are, $T_c = 1.321 \pm 0.004$ and $\rho_c = 0.306 \pm 0.001$ [14].

2. COMPUTATIONAL DETAILS

The Brownian Dynamics simulation technique is the same as we have used in previous studies (*e.g.*, [16]). A cubic simulation cell containing N LJ model molecules,

$$\phi(r) = 4\varepsilon\left(\left(\frac{\sigma}{r}\right)^{12} - \left(\frac{\sigma}{r}\right)^{6}\right) \tag{1}$$

was simulated. Two volume fractions, $\phi = \pi N\sigma^3/V$, where V is the volume of the simulation cell, is V, were considered $\phi = 0.05$ and 0.10. In each case an equilibrated system above the critical temperature, was quenched instantaneously to a temperature that placed it into the metastable/unstable two-phase region. Calculated properties are quoted in particle based reduced units, *e.g.*, σ for length, ε for energy, and a^2/D_0 for time, where $a = \sigma_{LJ}/2$ and D_0 is the self-diffusion coefficient of the colloidal particles of diameter σ_{LJ} in the limit of infinite dilution. $D_0 = k_B T/3\pi\eta_s\sigma$ where η_s is the viscosity of the solvent. The simulations and presented results are in these reduced units, and therefore conversion to specific systems would require real values for T,σ,η_s and ε.

The new feature of this work, when compared with our previous BD simulations is that we have carried out simulations of a non-equilibrium state as it approaches an equilibrium state. The system is perturbed by a temperature quench into the two-phase part of the LJ phase diagram, and its phase separation is monitored. The quench takes place in a single time step. In order to obtain improved statistics, the quenches were performed 5 times from statistically independent states at $T=2.0$ and the appropriate volume fraction. The equivalent quench responses were averaged for the purpose of presentation. Each quench was followed for typically $\sim 20a^2/D_0$ time units. Static and dynamic properties were evaluated at stages during the quench averaged over a consecutive series $0.82a^2/D_0$ time slices.

3. RESULTS AND DISCUSSION

A series of quenches was carried out into the two phase liquid-vapour and solid-vapour coexistence region of the LJ phase diagram, as illustrated in Figure 1. The quenches to $T=0.9$ and $T=0.7$ are in the liquid-vapour region, and the quench to $T=0.5$ is in the solid-vapour region. Following a quench, the homogeneous metastable or unstable state gradually phase separates into condensed phase and vapour regions. A typical example of such a process is shown in Figure 2 for the $\phi=0.1$ and $T=0.5$ state point using $N=864$. As can be seen in the figure, the initial homogeneous phase present at time $t=0$ gradually phase separates into high and low density regions.

After the temperature quenches, the development of local structure can be seen in the pair radial distribution function, $g(r)$, which shows a growth in the height of the first peak. Additional peaks also develop at $r\sim\sigma, 2\sigma\cdots$, indicative of some medium range ordering. Figure 3 presents radial distribution functions for a $T=2.0\rightarrow 0.7$ quench at $\phi=0.1$.

It is in many respects more informative to concentrate on the structure factors, $S(k)$, obtained by Fourier transformation of the $g(r)$, as it is better suited to discerning key distance scales. Examples of $S(k)$ at different times after a quench from $T=2.0\rightarrow 0.7$ at a mean volume fraction $\phi=0.1$ are presented in Figure 4. The signature of phase separaton is the appearance of a peak in $S(k)$ at very low wave vector $k\sim\sigma^{-1}$. (For a dense fluid in which excluded volume effects dominate, the first peak in $S(k)$ is at $k\sim 2\pi\sigma^{-1}$.) Both the inverse peak position, k_{max}^{-1}, which is a measure of the domain size and the peak height, $S(k_{max})$ indicate phase separation. At low volume fraction ($\phi=0.05$) both quenched temperatures ($T=0.7$ and $T=0.5$) for

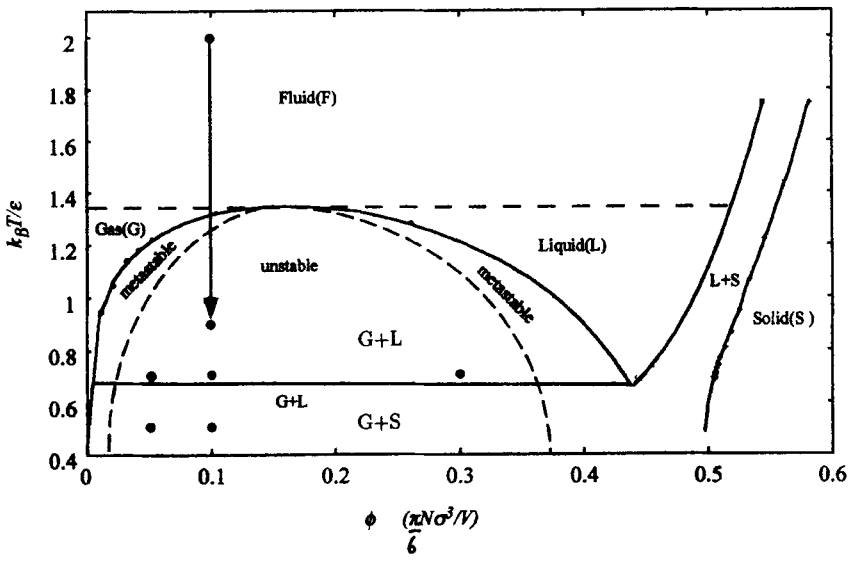

FIGURE 1 The Lennard-Jones phase diagram, showing quench final state points denoted by •. The estimated spinodal line is the $(\partial P/\partial \rho)_T = 0$ locus taken from the parameterised LJ equation of state of Johnson *et al.* [21]. The $G + S$ spinodal is not known with great certainty, and has been estimated by extrapolation of the $G + L$ spinodal.

$N = 256$ show an immediate decrease of peak position and an increase in the peak height, which is consistent with phase separation by spinodal decomposition. Being low density, they are fairly large systems, and are therefore less inclined to suffer from small system size induced latency (see below).

The peak position and height of the lowest k peak show evidence of a power law dependence with time,

$$k_{\max}^{-1} \propto t^{\alpha} \tag{2}$$

$$S(k_{\max}) \propto t^{\beta} \tag{3}$$

A summary of the α and β values obtained from these simulations is given in Table I and typical literature values in Table II. For $T = 0.7$ and $\phi = 0.05$ with $N = 256$ then $\alpha \sim 0.3 \pm 0.05$ at early times and $\alpha \sim 0.15 \pm 0.02$ at later times. This is consistent with a single atom evaporation/condensation

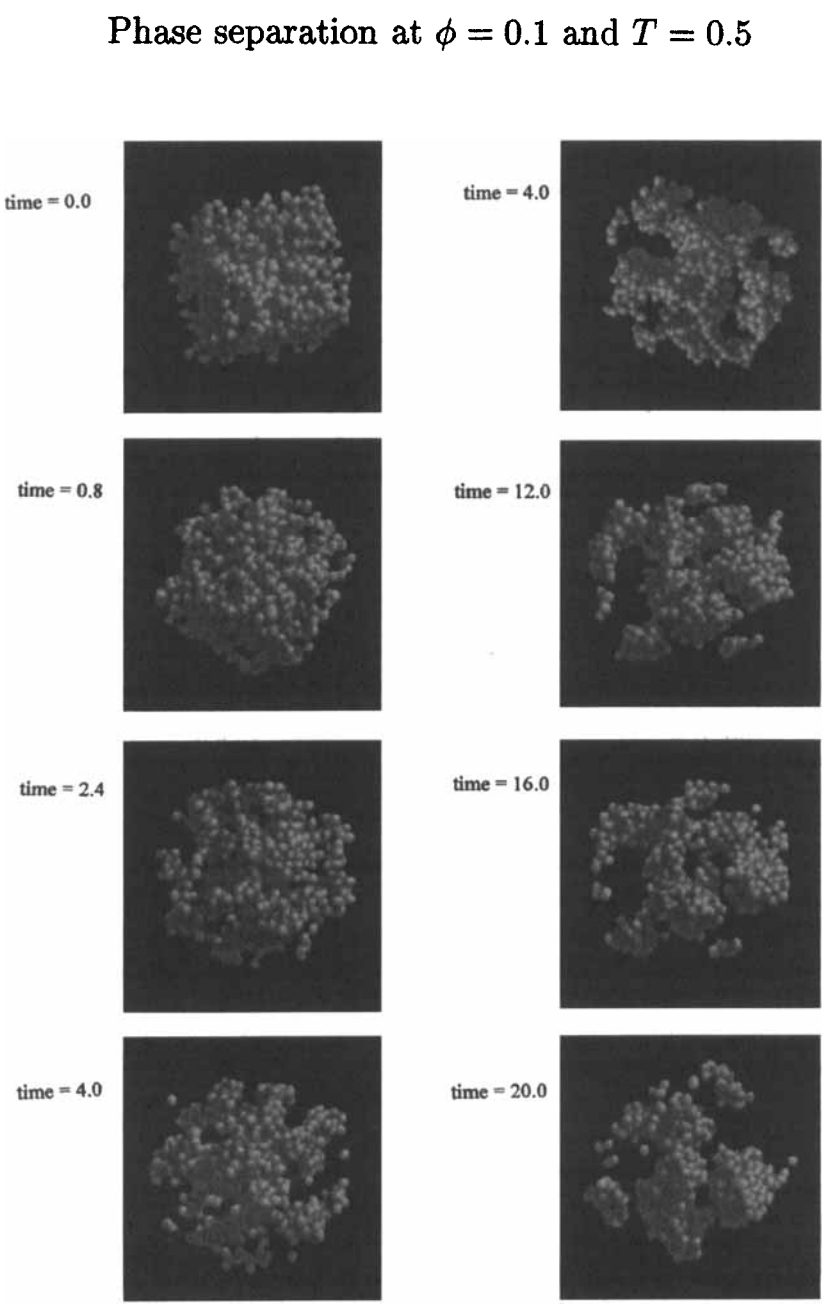

FIGURE 2 A series of perspective snapshots of a $N = 864$ and $\phi = 0.1$ LJ particles as a function of time resulting from a $T = 2.0 \rightarrow 0.5$ quench.

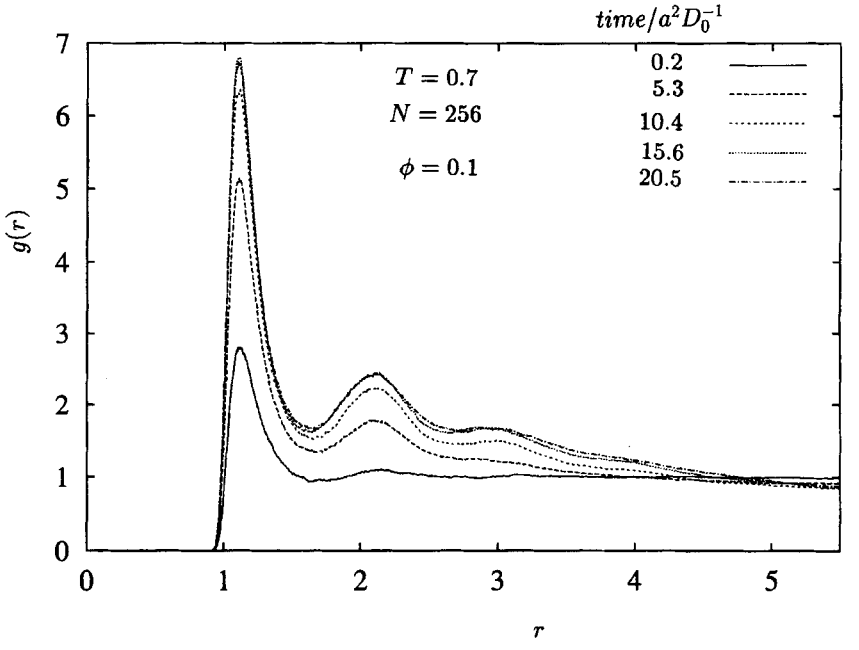

FIGURE 3 Radial distribution functions as a function of time for $\phi = 0.1$ and $N = 256$ and $T = 0.7$.

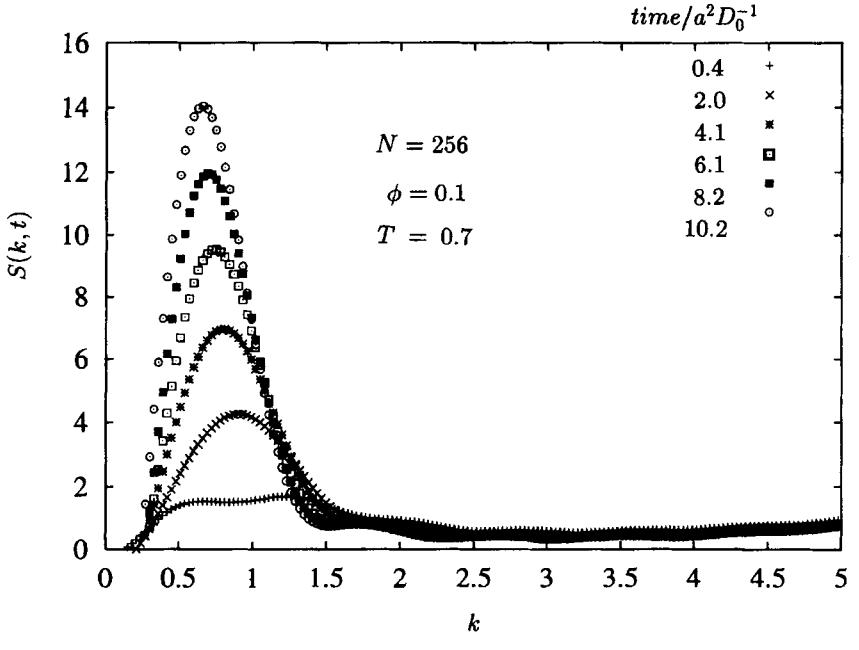

FIGURE 4 The structure factor as a function of time for the system of Figure 3.

TABLE I Summary of the states and growth power law exponents, assuming $k_{max}^{-1} \propto t^{\alpha}$, $S(k_{max}) \propto t^{\beta}$ and $u(t) \propto t^{\gamma}$. Uncertainties in the exponents are estimated to be $\pm$ 10%

ϕ	T	N	*Latency in* k_{max}^{-1}	*Latency in* $S(k_{max})$	α	β	γ
0.30	0.7	256	Yes	Yes	0.15→0.33	exp	–
0.30	0.7	500	No	Yes	0.33	exp	–
0.10	0.9	256	Yes	Yes	1.0	exp	–
0.10	0.7	256	Yes	Yes	0.5	0.5→0.95	–
0.10	0.5	256	No	Yes	0.34	0.75	0.22
0.10	0.7	864	No	No	0.19	0.70	0.17
0.05	0.7	256	No	No	0.3→0.15	0.9→0.6	0.25
0.05	0.5	256	No	No	0.21	0.75	0.34

TABLE II Literature values for the scaling growth law exponents α and β

Method	*Comments*	*reference*	α	β
Simulation	DLA	[2]	0.38–0.44	0.7–1.05
Simulation	LJ, MD	[3]	0.38	–
Experiment	Colloid	[5]	0.25→1	–
Experiment	Alloy, low ϕ	[1]	0.2–0.3	1.0
Experiment	Alloy, high ϕ	[1]	0.15	0.45
Theory	MF, Cahn, linear	[1]	0	exponential
Theory	MF, Lifshitz-Slyozov	[1]	0.33	–
Theory	MF, Siggia, surface tension driven	[10]	1.0	–
Theory	CD, Binder/Stauffer, cluster-cluster agg.	[20]	0.16	0.48

mechanism for cluster growth, moving to the slower dynamics of cluster-cluster amalgamation at later times. For the corresponding system, with $T = 0.5$, then we found that $\alpha \sim 0.21 \pm 0.02$ at all times. The Lyfshitz-Slyozov $t^{1/3}$ dynamics are only expected for small supersaturation. It is probable that at lower temperatures, small clusters are formed quickly, and therefore it is reasonable to expect the slower cluster-cluster coagulation dynamics to dominate at early times.

For the $T = 0.7$ quench at the higher mean volume fraction of 0.1, for $N = 256$ there is an initial latency in the decrease in k_{max} and in the increase of $S(k_{max})$. This suggests that growth by nucleation, rather than by spinodal decomposition (which would be expected at this point in the phase diagram) was the initial mechanism for the decay of the state. The latency period is followed by an increase in $S(k_{max})$, and then a decrease in k_{max} which did not follow an obvious power law. The change in the peak position with time took the form of a continuous increase in α, with perhaps a small region at intermediate time where $\alpha = 0.5$. The box size can have a significant effect on the phase separation of this system. It is long wavelength density

fluctuations which predominate at early times for the decomposition of unstable systems. If the simulation box is too small for these long wavelength fluctuations to exist, the system will have to phase separate via a nucleation-like mechanism, thus producing a latency period as seen in these results. A small box will also influence the rate of aggregation once it has started, making it easier for large clusters to grow. This leads to a rapid increase in the rate of growth which is evident in the behaviour of the structure factor. The periodic boundaries also affect the structure factor in that once $2\pi k_{\max}^{-1}$ approaches half the box sidelength, it will increase very rapidly until a peak is left at $k_{\max} \sim 0$ (a similar effect has been seen by Poon *et al.*, when a gel collapses [5]). The influence of the box size on the phase separation was confirmed by repeating the $T = 0.7, \phi = 0.1$ quench with a system of 864 particles. As revealed in Figure 5, this system showed immediate evidence of low wavelength decompostion with both the peak height and the peak position following power laws, in the latter case giving $\alpha = 0.19$. This is indicative of the slower growth dynamics expected for more concentrated systems. In contrast, the $N = 256$ system showed initial latency and then rapid growth of the clusters–a purely finite size effect. We have therefore demonstrated that system size can have a pronounced effect

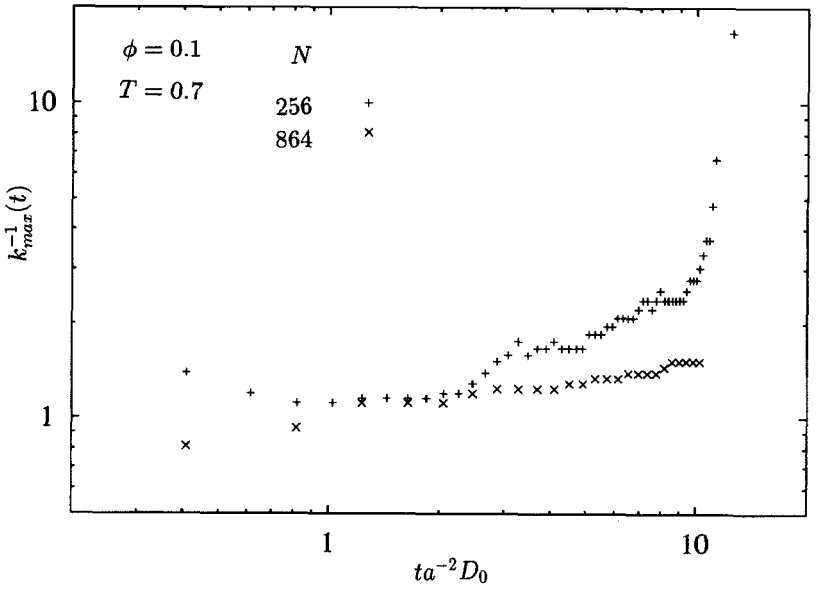

FIGURE 5 $k_{\max}^{-1}$ as a function of time for $\phi = 0.1$ and $T = 0.7$ for two different system sizes: $N = 256$ and $N = 864$.

on growth kinetics, and that at least $N \geqslant 864$ are advisable for studies of this kind.

For a 0.1 volume fraction $N = 256$ system quenched to $T = 0.9$ into the transitional region between metastable and unstable states, latency would be more likely since the quench was less deep and indeed this was observed. After this period, the peak height began to grow exponentially while the peak position remained constant, behaviour also seen in experimental studies of phase separation in colloid liquids [17]. Soon after this period of increase in peak height, the peak position also began to decrease and quickly collapsed to zero. This implies that a nucleation type mechanism was initiating the phase separation; however, it is to be expected that the simulation box size had a significant influence on the later stages of growth of these systems.

For the same volume fraction of 0.1 quenched to the lower temperature of 0.5, and using $N = 256$, the peak height increased immediately with power law behaviour although the peak position remained constant for a short time, after which it followed a power law decrease with $\alpha \sim 0.34$. The difference between a typical nucleation growth scenario ($N = 256, \phi = 0.1$ and $T = 0.9$) and spinodal decomposition growth ($N = 256, \phi = 0.05$ and $T = 0.5$) states is illustrated in Figure 6.

A very high volume fraction system was also considered, $\phi = 0.3$, at a temperature of $T = 0.7$ which also showed indications of size effects for systems 256 and 500 particles. In the smaller system there was a nucleation-like latency period before decomposition, and in both systems α increased fairly continuously through a small region of power law behaviour where $\alpha \sim 1/3$, to a very fast decrease of k_{max} to zero. However, these systems did not have power law behaviour of $S(k)$. Instead the $S(k)$ had exponential behaviour from the start in the larger system, and from the onset of decomposition in the smaller system. It is unclear at the moment if this is a system size induced feature or not.

The peak heights also show a power law growth with time. In fact, the power law dependence is in many respects better than for k_{max}^{-1}. In Figure 7, we show $S(k_{max}, t)$ for $\phi = 0.1$ and $T = 0.7$ quenches for $N = 256$ and $N = 864$. For the latter system size the power law behaviour is well followed. In Figure 8, $S(k_{max}, t)$ for the $\phi = 0.05$ quenches to $T = 0.5$ and $T = 0.7$ are shown (in both cases with $N = 256$). The power law exponent $\beta = 0.8 \pm 0.1$ seems to be relatively insensitive to the state point points we considered.

The thermodynamic quantity, the interaction energy per particle, u,

$$u = \frac{1}{N} \sum_{i=1}^{N-1} \sum_{j=i+1}^{N} \phi_{ij} \tag{4}$$

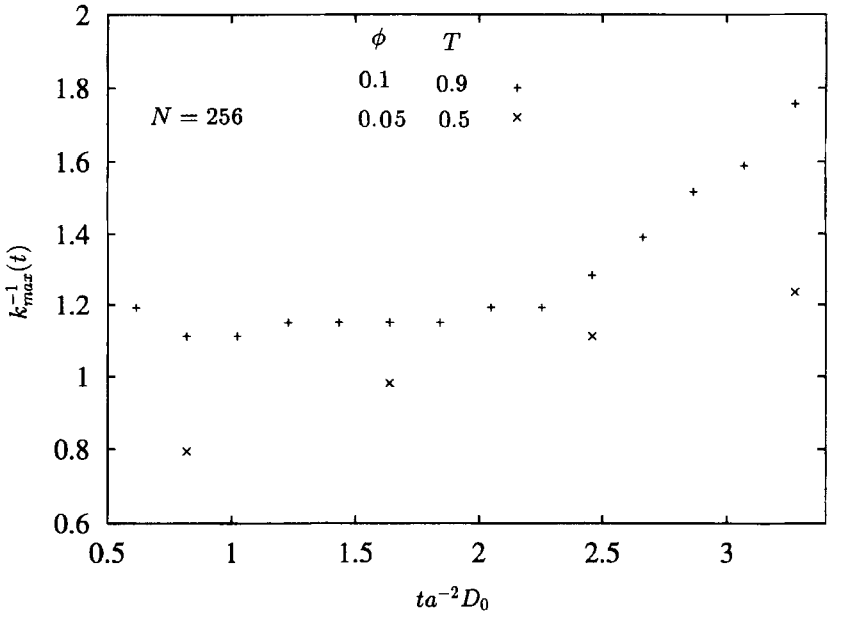

FIGURE 6 k_{max}^{-1} as a function of time for states showing classical nucleation ($T = 0.9$) and spinodal decomposition ($T = 0.5$) behaviour.

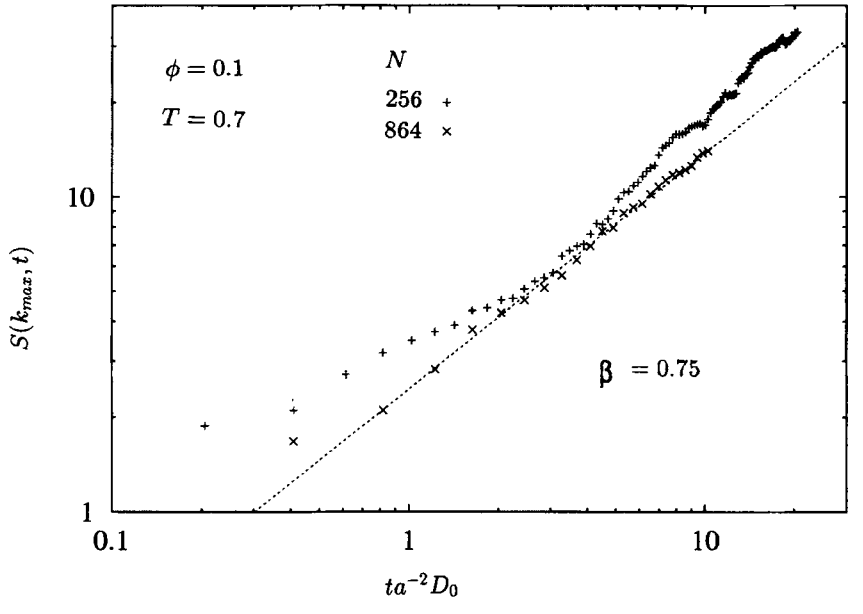

FIGURE 7 $S(k_{max}, t)$ as a function of time for two different system sizes at a mean volume fraction of 0.1 and temperature of 0.7.

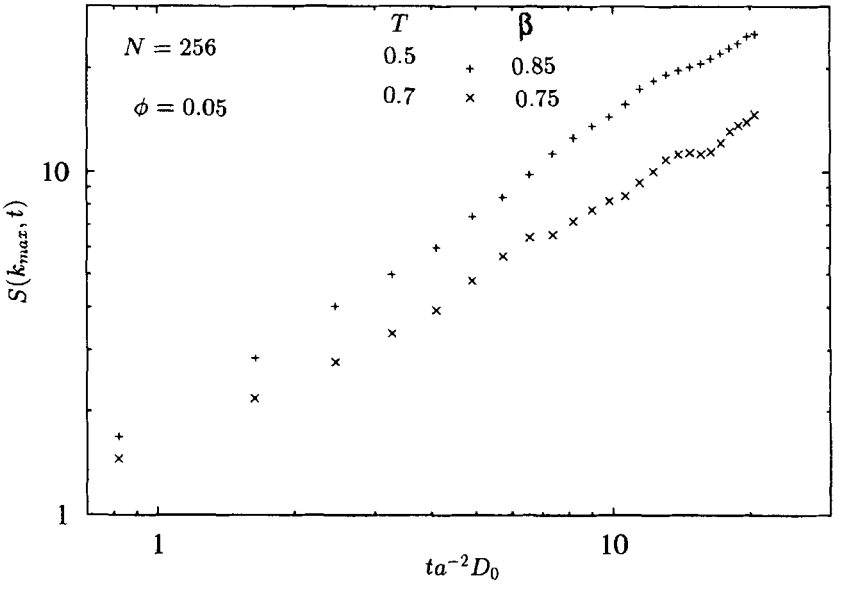

FIGURE 8 $S(k_{max}, t)$ as a function of time for $\phi = 0.05$ and (a) $T = 0.5$ and (b) $T = 0.7$.

was also followed as a function of time. This property becomes more negative with time as the particles associate more closely and also decreases with temperature, reflecting the increased level of association that takes place in this part of the phase diagram. $u(t)$ also shows a power law growth,

$$u(t) \propto t^{\gamma} \tag{5}$$

Some examples of this growth are given in Figures 9 and 10. The exponent is typically 0.2 ± 0.1. The interaction energy, which reflects the local density of particles, was also found to evolve with power law behaviour. As temperature decreases, γ increases, which is representative of the stronger particle interactions at lower temperatures causing denser clusters to be formed. Perhaps less intuitively, γ decreases as the volume fraction increases. This can be explained by considering the proximity of clusters to each other at different mean volume fractions. At low volume fractions, clusters are more independent of each other, and therefore the interparticle forces experienced by particles in a cluster will be from that cluster alone (to a very good approximation) which pull it tighter together. At higher volume fractions, the potential field from particles in surrounding clusters penetrate

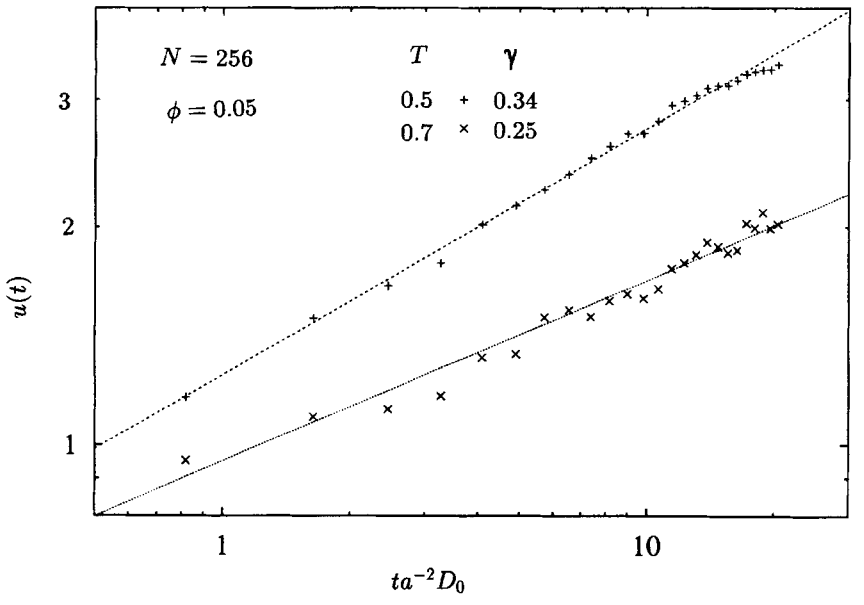

FIGURE 9 The average interaction energy per particle for the states of Figure 8.

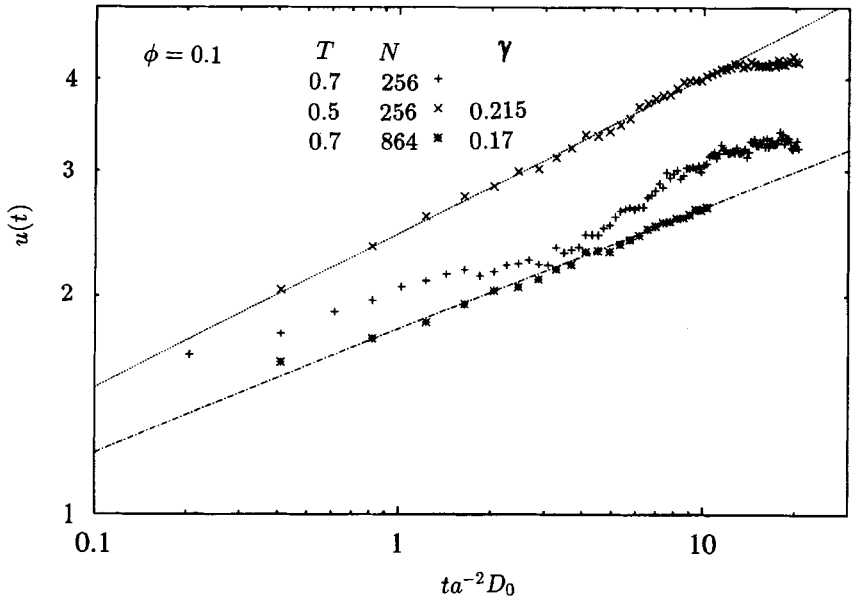

FIGURE 10 As for Figure 9, except that the system size dependence of $u(t)$ is explored.

each cluster. This opposes the forces between the particles in the cluster, causing the cluster to adopt a more diffuse structure. This could produce a slower rate of cluster densification with time for the higher volume fraction systems.

Up to this point we have been concerned with the time evolution of static properties in the two phase region. Truly dynamical properties (*e.g.*, self-diffusion coefficients and shear viscosity) themselves evolve during this process. Indeed, the change in these properties is the most obvious manifestation of phase separation at intermediate ('gel') times in aggregating colloidal systems. With the mean square displacements, time origins, t_0, commenced at a selection of times separated by 0.8 reduced time units in the phase separation, displayed mean square displacements, msd(t) that depended on time according to the general law,

$$\text{msd}(t - t_0) \propto (t - t_0)^{\theta(t_0)} \tag{6}$$

where the exponent, θ, decreased with time, t, from the start of the quench. Examples of $\theta(t_0)$ are presented in Figure 11 for $\phi = 0.1$ and $N = 256$ states. The figure shows that $\theta(t_0)$ decreases with time, at a greater rate for the lower final quench temperatures. The lack of a linear regime in the mean square displacements causes a practical problem in computing time dependent transport coefficients in the domain separating regime. The transport coefficient changes with time more rapidly than the time required by conventional procedures to calculate it; in this case, the long-time self-diffusion coefficient. The decrease in $\theta(t_0)$ with time reflects the decrease in the self-diffusion coefficient during the phase separation. Traditional routes to the long time self-diffusion coefficient do not appear to be very useful in these quenched systems, as the system evolves in its physical state at a rate that is much greater than the time required to compute the transport coefficient. It is an intriguing question, therefore, whether it is possible to compute the long-time self-diffusion as a function of time in these systems; and is D a meaningful quantity in this context?

We also computed the shear-stress time autocorrelation function, $C_s(t)$,

$$C_s(t) = \frac{V}{k_B T} \langle \sigma_{xy}(0)\, \sigma_{xy}(t) \rangle, \tag{7}$$

where $\langle \cdots \rangle$ indicates an average over time origins in Eq. (7). The stress tensor, $\underline{\sigma}$, in this Rouse level model is written solely it terms of the thermo-

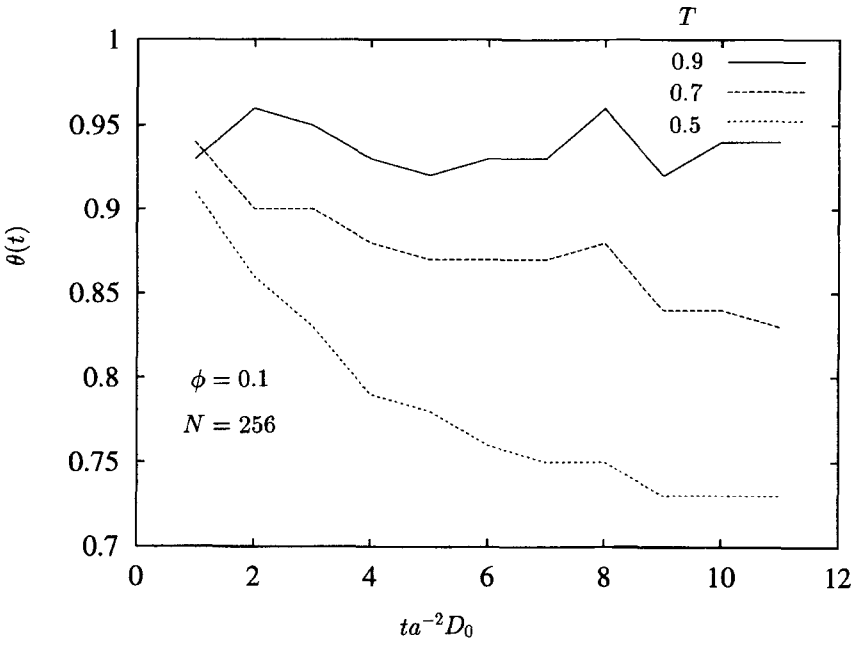

FIGURE 11 Time dependence of the mean square displacement exponent, θ for $\phi = 0.1$ systems at a selection of quench temperatures, which are given on the figure.

dynamic interactions between the particles.

$$\underline{\sigma} = \frac{\rho}{N} \sum_{i=1}^{N-1} \sum_{j=i+1}^{N} (\underline{r}_{ij} \underline{r}_{ij} / r_{ij}) V'_{ij} \tag{8}$$

The interaction part of the shear viscosity is given by,

$$\eta_0 = \int_0^\infty C_s(t) dt \tag{9}$$

The viscosity is conveniently normalised by the solvent viscosity η_s.

Figure 12 shows $C_s(t)$ computed from a stream of stress values up to times given on the label key of the figure, to a resolution of 2 reduced time units. The correlation functions show increasingly slow relaxation with time from the start of the quench. In fact, except for the first few curves computed from stress values at $tD_0/a^2 < 3$, complete relaxation does not occur in the simulation time. One can identify the limiting stress values at $t \sim 0.3$

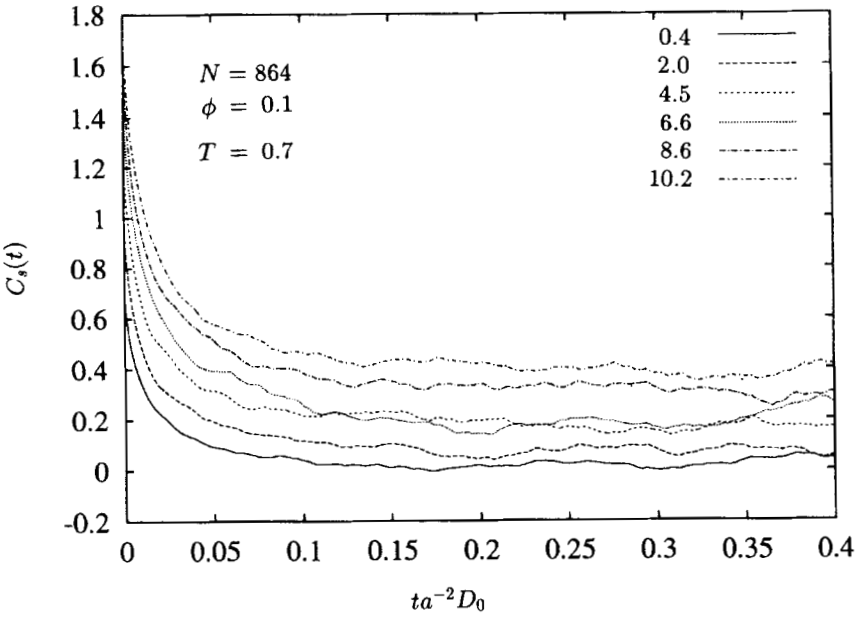

FIGURE 12 Time dependence of the shear stress autocorrelation function $C_s(t)$ in periods after the quench and annotated on the figure.

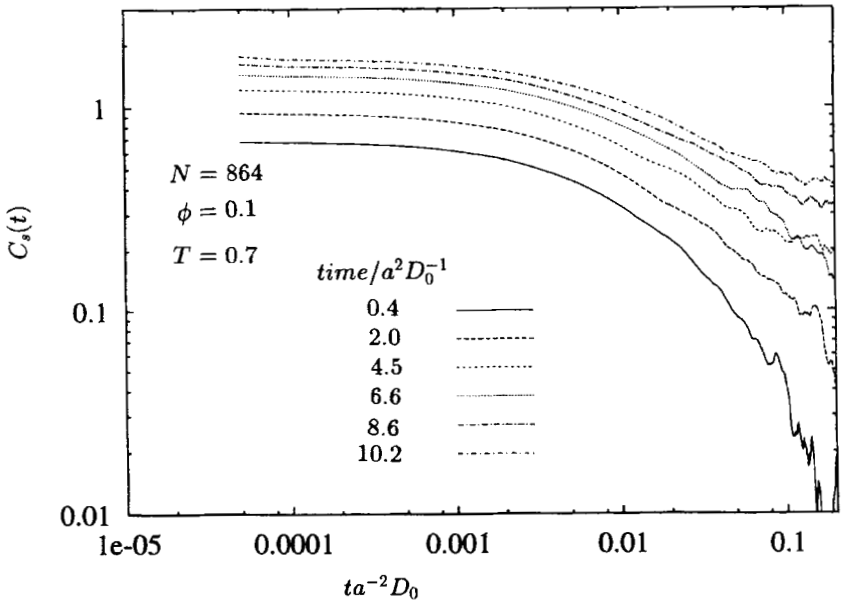

FIGURE 13 $\log(-\log(C_{sn}(t)))$ *vs.* $\log(t)$ for an $N = 864$ quench at $\phi = 0.1$ and $T = 0.7$.

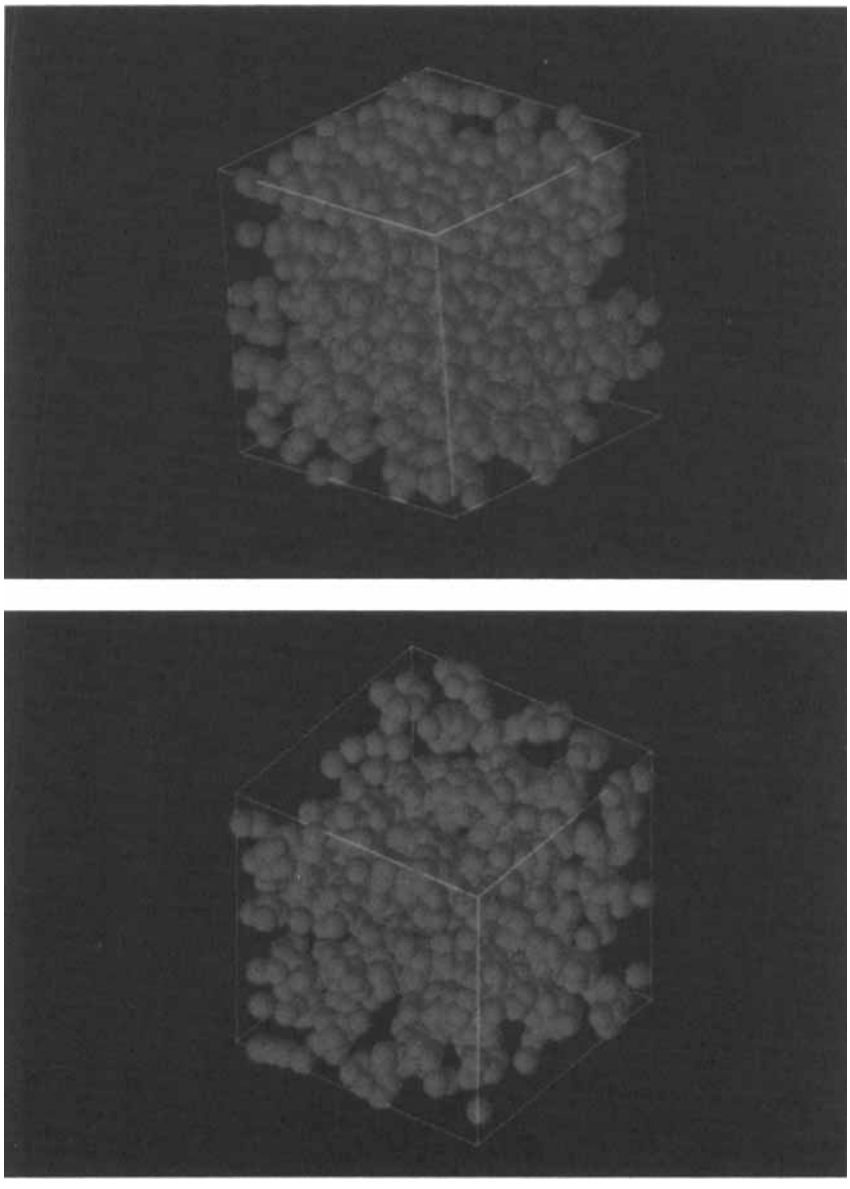

FIGURE 14 A series of perspective snapshots of a $N = 864$ and $\phi = 0.05$ LJ particle system as a function of time after a $T = 2.0 \rightarrow 0.3$ quench in one time step. Key: times from the start of the quench in $a^2 D_0^{-1}$ (a) 0.0, (b) 0.82, (c) 4.10, (d) 8.19, (e) 12.29 and (f) 20.48. See Color Plate I.

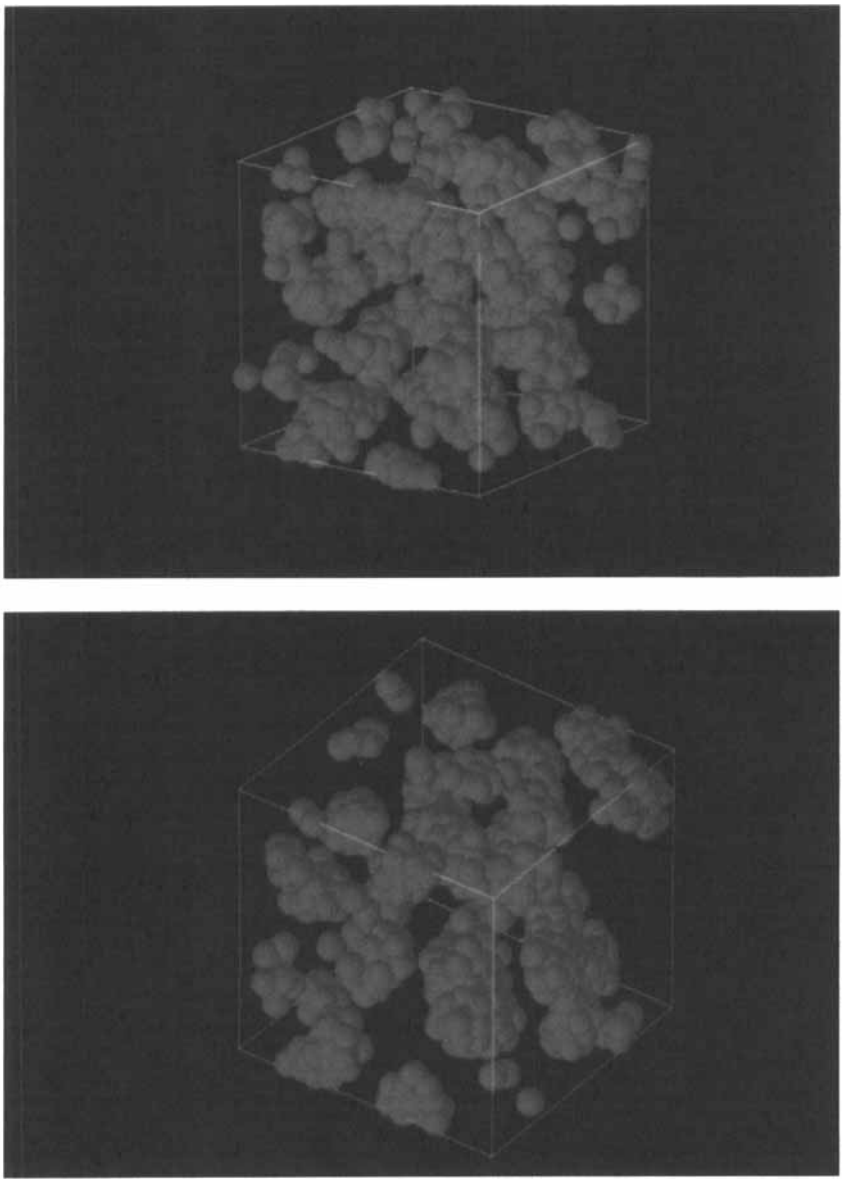

FIGURE 14 Continued.

as being the long-time shear moduli, reflecting the rigidity of a percolating gel-like network. As for the self-diffusion coefficient, we do not yet have a convenient method of computing the time dependence of the viscosity of the

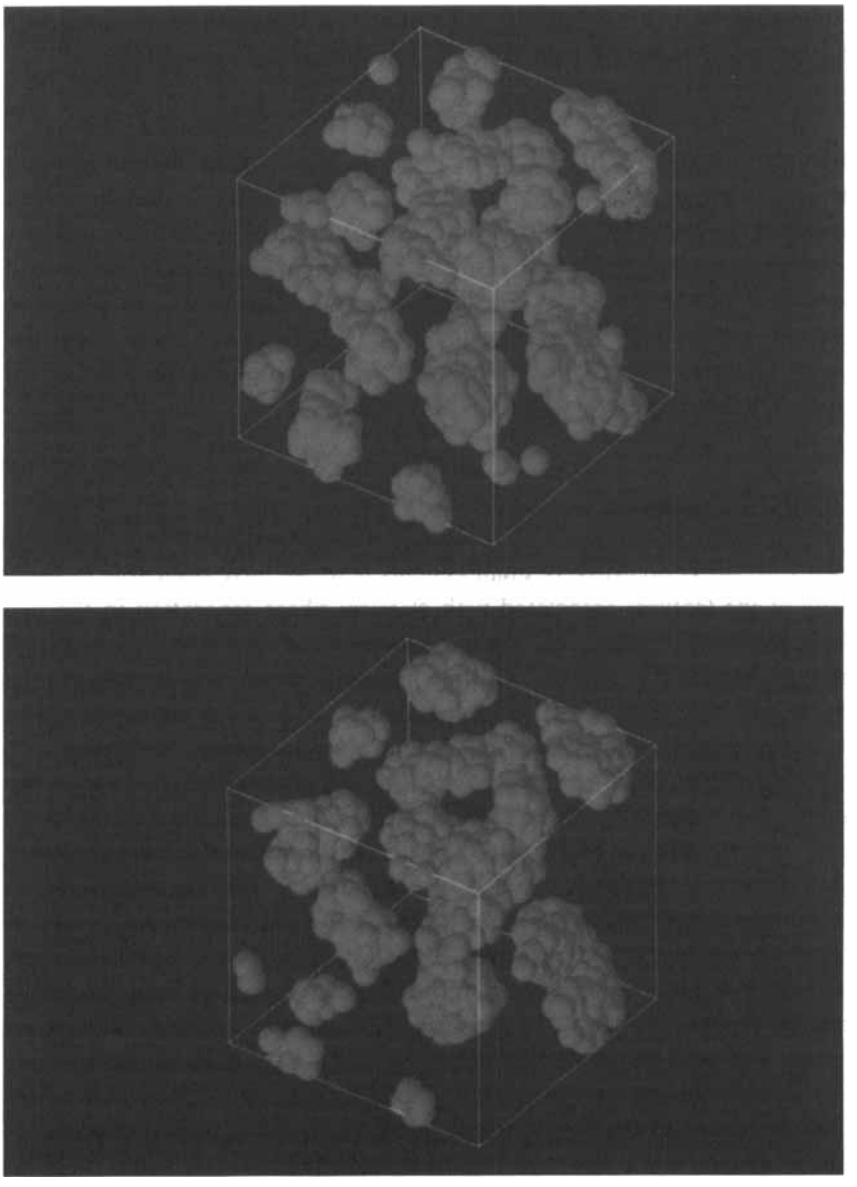

FIGURE 14 Continued.

system through the period of phase separation. The system evolves too quickly, at a rate faster than is required for the stress correlation function to decay to zero.

The analytic form of $C_s(t)$ has been used as a signature for the approach of gelation. A transition from a fractional exponential form, [18]

$$C_s(t) = G_\infty \exp(-(t/\tau')^\beta), \tag{10}$$

to an alebraic decay $C_s(t) \sim t^{-v}$ where v is an exponent, is thought to mark the transition to a gel state in which a self-similarity in time scales is considered to hold [19]. We find that at short times after the quench, decay is stretched exponential, whereas the correlation functions increasingly tend towards a power law decay as phase separation proceeds. An algebraic decay is indicated by a linear region in $\ln(C_s(t))$ *vs.* $\ln(t)$, with slope $-v$. Figure 13 shows $C_s(t)$ evaluated in time bands given on the key label of the figure. The limiting slope at long time, $v \sim 0.5$.

4. CONCLUSIONS

Even with the comparitively small systems here, we have been able to show many of the features associated with classical phase separation in the two phase region. The structural, thermodynamic and transport properties all show a power law variation with time. Domain growth was revealed in the appearance of a peak in the structure factor at $k_{max} \sim \sigma_{LJ}^{-1}$ which moved to lower k with time, and whose peak height $S(k_{max})$ increased with time. k_{max}^{-1} and $S(k_{max})$ show a power law dependence with time with exponents in the range 0.2–0.3 and 0.7–1.0, respectively. The kinetics of domain growth, as characterized by these exponents, depends on the value of temperature and mean density quenched to in the two-phase region. For quenches close to the liquid-vapour coexistence line, an initial period marked by a lack of growth in the low k peak ('latency') is followed by power law behaviour, which is indicative of growth by nucleation. Quenches to well inside the unstable region are marked by classical spinodal decomposition power law growth. The influence of the simulation cell size on the phase separation has been investigated by carrying out simulations with $N = 256$ and $N = 864$. Small system sizes tend to promote latency and more rapid phase separation at longer times, although intermediate time behaviour does still compare well with theoretical predictions.

Network formation is manifest in a slowing down in relaxation processes marked by a decrease in the self-diffusion coefficient and increase in shear viscosity with time from the start of the quench. The shear stress time correlation function was evaluated at various times during the phase separation. These indicate that a percolating phase with significant long-time rigidity was

forming, a feature identified with the gel state. As yet, the simulations have not been extended to long enough times to ascertain whether this gel-like 'metastable' structure will eventually phase separate or whether it remains in this 'pinned' state.

Acknowledgement

JFL thanks the EPSRC for a research studentship.

References

[1] Gunton, J. D., San Miguel, M. and Sahni, P. S. (1983) in *Phase Transitions and Critical Phenomena*, ed. Domb C. and Lebowitz J. L. (Academic, London), Ch. 3, **8**, 267–482.
[2] Haw, M. D., Sievwright, M., Poon, W. C. K. and Pusey, P. N. "Structure and characteristic length scales in cluster-cluster aggregation simulation", *Physica A* **127**, 231–260.
[3] Mruzik, M. R., Abraham F. F. and Pound, G. M. (1978). *J. Chem. Phys.*, **69**, 3462.
[4] Koch, S. W., Desai R. C. and Abraham F. F. (1983) "Dynamics of phase separation in two-dimensional fluids: spinodal decomposition", *Phys. Rev. A* **27**, 2152–2167.
[5] Poon, W. C. K., Pirie, A. D. and Pusey, P. N. (1995) "Gelation in colloid-polymer mixtures", *Faraday Disc.*, **101** in press.
[6] Bastea, S. and Lebowitz, J. L. (1995) "Comment on 'Phase separation in two-dimensional fluid mixtures'", *Phys. Rev. Lett.*, **75**, 3776.
[7] Binder, K. (1987) "Theory of first order phase transitions", *Rep. Prog. Phys.*, **50**, 783–859.
[8] Tanaka, H., Yokawa, T., Abe, H., Hayashi, T. and Nishi, T. (1990) "Transition from metastability to instability in a binary liquid mixture", *Phys. Rev. Lett.*, **65**, 3136–3139.
[9] Bray, A. J. (1994) "Theory of phase-ordering kinetics", *Adv. in Physics*, **43**, 357–459.
[10] Siggia, E. D. (1979) "Late stages of the spinodal decomposition in binary mixtures", *Phys. Rev. A*, **20**, 595–605.
[11] Anhuwalia, R. and Puri, S. (1996) "Phase ordering dynamics in binary mixtures of surfactants", *J. Phys.: Condens. Matt.*, **8**, 227–244.
[12] Laradji, M., Mouritsen, O. G., Toxvaerd, S. and Zuckermann, M. J. (1995) "Molecular dynamics simulations of phase separation in the presence of surfactants", *Phys. Rev. E*, **50**, 1243–1252.
[13] Zhu, P. W. and Napper, D. H. (1994) "Studies of aggregation kinetics of polystyrene latices sterically stabilized by poly(*N*-isopropylacrylamide)", *Phys. Rev. E*, **50**, 1360–1366.
[14] Kofke, D. A. (1993) "Direct evaluation of phase coexistence by molecular simulation via integration along the saturation lime", *J. Chem. Phys.*, **98**, 4149–4162.
[15] Agrawal, R. and Kofke, D. A. (1995) "Thermodynamic and structural properties of model systems at solid-fluid coexistence II. Melting and sublimation of the Lennard-Jones system", *Mol. Phys.*, **85**, 43–59.
[16] Mitchell, P. J., Heyes, D. M. and Melrose, J. R. (1995) "Brownian-dynamics Simulations of model stabilised colloidal dispersions under shear", *JCS Farad. Trans.*, **91**, 1975–89.
[17] Pusey, P. N., Pirie, A. D. and Poon, W. C. K. (1993) "Dynamics of colloid-polymer mixtures", *Physica A*, **201**, 322–331.
[18] Heyes, D. M. and Mitchell, P. J. (1994) "Self-diffusion and viscoelasticity of dense hard-sphere colloids", *JCS Farad Trans.*, **90**, 1931–1940.
[19] Michon, C., Cuvelier, G. and Launay, B. (1993) "Concentration dependence of the critical viscoelastic properties of gelatin at the gel point", *Rheolog. Acta.*, **32**, 94–103.
[20] Binder, K. and Stauffer, D. (1974) "Spinodal decomposition of binary mixtures", *Phys. Rev. Lett.*, **33**, 1006–1009.
[21] Johnson, J. K., Zollweg, J. A. and Gubbins, K. E. (1993) "The Lennard-Jones equation of state revisited", *Molec. Phys.*, **78**, 591–618.